

Original Article

Cite this article: Wabo H, De Kock MO, Beukes NJ, and Hegde VS (2022) Palaeomagnetism of the uppermost carbonate units of the Purana basins in southern India: new demagnetization results from the Kaladgi and Bhima basins, Karnataka. *Geological Magazine* **159**: 269–278. <https://doi.org/10.1017/S0016756820001181>

Received: 7 January 2020

Revised: 15 June 2020

Accepted: 6 October 2020


First published online: 19 November 2020

Keywords:

southern India; Purana basins; unconformity-bound Sequence III; carbonates; palaeomagnetism

Author for correspondence: Herve Wabo, Email: hwabo@uj.ac.za

Palaeomagnetism of the uppermost carbonate units of the Purana basins in southern India: new demagnetization results from the Kaladgi and Bhima basins, Karnataka

Herve Wabo¹ , Michiel Olivier De Kock¹, Nicolas Johannes Beukes¹ and Venkatraman Seetaram Hegde²

¹Department of Science and Innovation, National Research Foundation, Centre of Excellence for Integrated Mineral and Energy Resource Analysis (DSI-NRF CIMERA) and Paleoproterozoic Mineralization Research Group (PPM Research Group), Department of Geology, University of Johannesburg, PO Box 524, Auckland Park 2006, Johannesburg, South Africa and ²Civil Engineering Department, Sri Dharmasthala Manjunatheshwara (SDM) College of Engineering and Technology, Dharwar 580 002, Karnataka, India

Abstract

Four unconformity-bound sequences can be identified in the Purana successions in southern India, of which the third sequence (Sequence III) has the widest distribution. Sequence III contains deep-water carbonate units with consistent sedimentological characteristics across the subcontinent. The current extent of field relationships and existing ages has not allowed the correlation and chronology of these carbonates to be established conclusively. Palaeomagnetism may help resolve this essential question for the Purana sedimentation. Here, we report new palaeomagnetic results (HIG+/- pole: 21.7° N, 81.1° E, radius of cone of 95% confidence $A_{95} = 15.9^\circ$) from Sequence III carbonates in the Kaladgi (Badami Group) and Bhima (Bhima Group) basins. The HIG+/- magnetization, revealed after the removal of secondary magnetizations that include a present-day field and an Ediacaran–Cambrian overprint, is interpreted to be primary based on its dissimilarity to known younger magnetizations, the presence of distinctly different magnetic components in sites and a positive reversal test. Our HIG+/- pole differs from the *c.* 1.4 Ga pole and various *c.* 1.1 Ga and younger poles. Instead, it overlaps with the Harohalli dyke pole that was long considered to be *c.* 823 Ma in age, but has recently been suggested to be much older with an age of *c.* 1192 Ma. We therefore consider the uppermost carbonate beds of Badami and Bhima groups to have been deposited during late Mesoproterozoic times. A critical evaluation of parameters from which an earlier Neoproterozoic age for these carbonates was established indicates that the available ⁴⁰Ar/³⁹Ar, Rb–Sr and U–Pb ages in the Kaladgi and Bhima basins could reflect the timing of post-depositional alteration events.

1. Introduction

Proterozoic supracrustal successions, preserved in the so-called ‘Purana basins’ (e.g. Kale & Phansalkar, 1991; Chaudhuri *et al.* 1999, 2002; Chakraborty *et al.* 2010; Meert & Pandit, 2015), cover large parts of the Dharwar, Bastar and Singhbhum cratons of the India Shield south of the Indian Central Tectonic Zone (Fig. 1a). On purely stratigraphic grounds, the strata in these basins display a very similar development with four unconformity-bound sequences (Sequences I, II, III and IV) present (e.g. Conrad *et al.* 2011) of which the third (i.e. Sequence III) is the focus of this study in the Kaladgi and Bhima basins (see Fig. 1b). Sequence III, with a thickness of about one hundred to a few hundred metres, has the widest distribution of the four sequences. It rests directly on the Archean basement in some areas, such as in the far eastern Indravati and Chattisgarh basins as well as in the Bhima Basin to the west (Fig. 1b). Sequence III also has a very persistent internal stratigraphy and character, with a sharp erosional base overlain by conglomerate and quartzite fining upwards into shale, and finally into a very distinctive upper succession of finely laminated non-stromatolitic deep-water, largely pelagic, limestone and dolomite (e.g. Mukhopadhyay & Chaudhuri, 2003; Patranabis-Deb *et al.* 2012). This carbonate-rich unit also appears to have a distinctive laterally correlatable internal stratigraphy, with a middle siliciclastic unit (shale with minor quartzite) and an uppermost shale (Fig. 1b) overlain with erosional contact by siliciclastics of Sequence IV comprising the Sullavai Group and correlatives (e.g. Saha *et al.* 2016). Apart from its apparent lateral persistent stratigraphy, the strata of Sequence III also differ from those of underlying Sequences I and II by being virtually undeformed and almost flat-lying (e.g. Saha *et al.* 2016). The erosional unconformity at the base of Sequence III therefore varies along-strike from a subtle low angle to marked steep angle.

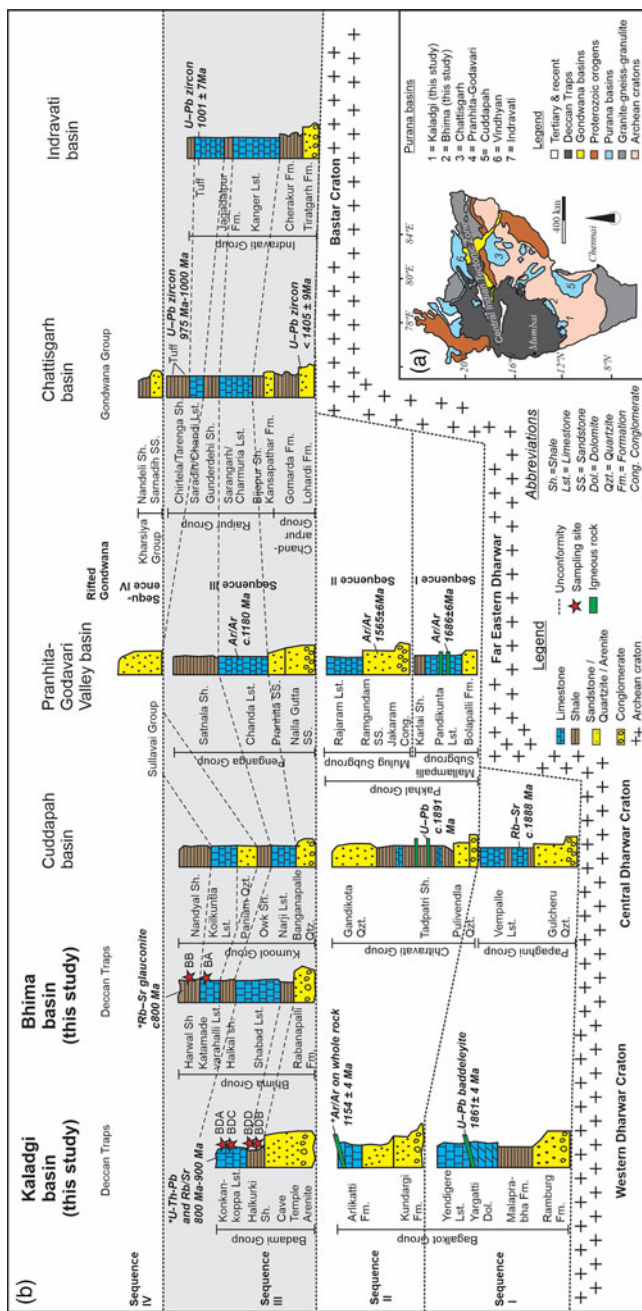


Fig. 1. (a) Simplified geological map of India showing the locality and outcrop distribution of the different Purana basins, the Gondwana Supergroup and the Deccan Traps (modified from Dey, 2015). (b) General stratigraphy of the different Purana basins with existing absolute age constraints (modified from Conrad *et al.* 2011; Collins *et al.* 2015; Meert & Pandit, 2015) showing the four unconformity-bound sequences. Carbonates of Sequence III (shaded) display very similar stratigraphic and sedimentological features that are apparently correlative across the subcontinent. Sampling sites are indicated. Age constraints with asterisk are discussed in the text.

Despite the apparent consistency of stratigraphy and sedimentological characteristics of Sequence III as depicted in Figure 1b, especially the persistence of deep-water carbonate units, there are still contrasting long-distance correlations. For example, in two of the most recent publications, this sequence in the Cuddapah and Kaladgi–Bhima basins are interpreted by Collins *et al.* (2015) and Joy *et al.* (2018) as early Neoproterozoic in age, while it is considered to be late Mesoproterozoic in age further to the east in the Pranhita,

Chattisgarh and Indravati basins. This discrepancy is essentially related to the interpretation of available radiometric age data of rock units in Sequence III. Arguably, the most robust age bracket for this sequence comes from the Chattisgarh Basin (Fig. 1b), where zircons extracted from tuff beds near its base and top indicate deposition between *c.* 1.4 Ga and *c.* 1.0 Ga (Patranabis-Deb *et al.* 2007; Bickford *et al.* 2011). The early Neoproterozoic age of Sequence III further to the west is based on a single outlier near-concordant U–Pb age of *c.* 0.91 Ga (Collins *et al.* 2015) obtained on detrital zircons extracted from the middle quartzite (i.e. Paniam Quartzite) of the succession in the Cuddapah Basin. The other detrital zircons, however, showed a much older and quite prominent peak at *c.* 1.7 Ga (Collins *et al.* 2015). In the Kaladgi and Bhima basins (the subject of this study), the Neoproterozoic age of Sequence III is based on U–Th–Pb and Rb–Sr ages of *c.* 800–900 Ma obtained on glauconite and limestone (Joy *et al.* 2018). However, the outlier zircon age and glauconite ages must be treated with care; Conrad *et al.* (2011) suggested that in the Pranhita and Chattisgarh basins these minerals were most likely reset, as they gave ages younger than the *c.* 1.0 Ga zircons in the upper tuff bed of the sequence (Fig. 1b).

With reference to the above, the stratigraphic correlation of Sequence III as presented in Figure 1b and the ages determined from glauconites and limestones (Joy *et al.* 2018) therefore remain unresolved. Another method that could be used to obtain more clarity on this question is that of palaeomagnetism. Such studies can yield insights into the lateral correlation and timing of deposition of deep-water carbonate units of Sequence III by comparing their remanent primary magnetization in the different Purana basins with existing results from dated Indian rock units. Additionally, information about the palaeogeographic setting of the southern Indian Shield during the Purana sedimentation can be constrained. However, a review of the palaeomagnetic database reveals that, except for the Pranhita–Godavari and Chattisgarh basins, from which De Kock *et al.* (2015) obtained a well-constrained palaeopole, there is a lack of robust data for the carbonates in Sequence III of the Purana basins. Here, we report new palaeomagnetic results for these carbonates in the Kaladgi and Bhima basins.

2. Regional geology

Outcrops of the Purana successions in the Kaladgi Basin cover about 8500 km² of the *c.* 400 000 km² Dharwar craton, and consist of shallow-marine sediments of thickness *c.* 4 km (e.g. Dey, 2015) that can be subdivided into the *c.* 3600-m-thick older Bagalkot Group and the *c.* 300-m-thick younger Badami Group, indicated here as part of Sequence III based on purely lithostratigraphic correlation (Fig. 1b). The virtually undeformed strata of the Badami Group overly deformed strata of the Bagalkot Group with sharp angular unconformity. The Badami Group comprises the basal Kerur Formation composed of conglomerate and quartzite, and the overlying Katageri Formation (e.g. Dey, 2015). The Katageri Formation includes the Halkurki Shale and the Konkankoppa Limestone, which are the subjects of this study (Fig. 1b).

The Bhima Basin (Fig. 1b) is developed adjacent to the Kaladgi Basin and covers *c.* 5200 km² of the Dharwar Craton (e.g. Dey, 2015). The succession in the basin is referred to as the Bhima Group and is subdivided into two formations: a lower siliciclastic Rabanpalli Formation and an upper limestone and shale Shahabad Formation (Fig. 1b). The Bhima Group is similar in appearance to the Badami Group of the immediately adjacent Kaladgi Basin, and is correlatable with it on lithostratigraphic grounds (Fig. 1b).

3. Sampling and methodology

For this study, a total of 49 oriented cores were collected from the Konkankoppa Limestone (sites BDA and BDC) and the Halkurki Shale (sites BDB and BDD) of the Badami Group in the Kaladgi Basin (Fig. 1b), and from the Katamdevarahalli Limestone (BA) and the Harwal Shale (BB) of the Bhima Group in the Bhima Basin (Fig. 1b). Individually oriented cores (33 cores in the Kaladgi Basin and 16 cores in the Bhima Basin) were collected *in situ* using a portable, hand-held petrol drill. We avoided hill exposures in order to minimize the risk of isothermal remanent magnetizations masking older magnetizations. In both basins, the limestone and shale that was sampled appeared finely laminated and of a deep-water below-wave-base depositional setting. We did not identify any conglomerates or rip-up clasts in any of the sampled units and this, combined with the virtually undeformed flat-lying nature of the beds, prohibited direct *in situ* conglomerate and/or fold stability tests.

Seven to nine oriented cores were collected from each of the six sites. Individual cores were oriented using a magnetic compass as well as a sun compass. No discrepancy between the magnetic and sun compass readings was observed.

The oriented cores were cut into *c.* 2-cm-long samples and subjected to stepwise demagnetization. Each core provided one sample. All measurements were made with a vertical 2G Enterprises DC-4 K superconducting rock magnetometer with an automated sample changer (Kirschvink *et al.* 2008) housed at the University of Johannesburg. Following a measurement of natural remanent magnetization and low-field-strength alternating-field (AF) cleaning of samples in four 2.5 mT steps up to 10 mT, the samples were thermally demagnetized in an ASC TD48-SC shielded furnace. Thermal demagnetization was achieved by heating samples at decreasing intervals from above 100°C until the magnetization of samples dropped below the noise level of the sample handler (*c.* 70 nAm²). Magnetic components were identified and quantified via least-squares principal component analysis (Kirschvink 1980) utilizing Paleomag 3.1.0 (Jones 2002). All visualizations of calculated palaeopoles utilized GPlates 2.1 (Williams *et al.* 2012). For interpretation of the references to colour in figures, the reader is referred to the version of this article published online.

4. Demagnetization results

4.a. Badami Group of the Kaladgi Basin

Stepwise (AF and thermal) demagnetization of sites BDB and BDD in the Halkurki Shale and BDA and BDC from the conformably overlying Konkankoppa Limestone revealed distinct magnetic components with variable stability (Figs 2, 3; Table 1).

The first component to unblock was revealed during the AF pretreatment in all sites, and persisted in most cases up to thermal demagnetization steps of 200–250°C (Fig. 2; Table 1). This low-stability magnetization, oriented north with a positive inclination, is comparable to the local present-day field, and is therefore denoted PDF (Fig. 3). Following the removal of PDF at site BDD, an intermediate unblocking component, denoted INT1+, was observed between temperature steps of 250°C and 300°C (Fig. 2). It consisted of a relatively well-grouped northerly set of directions with very shallow inclinations (Fig. 3; Table 1). INT1+ was also identified at site BDC, but there it represents a characteristic remanent magnetization (ChRM) that is unblocked by *c.* 530°C (Figs 2, 3; Table 1).

The ChRM of site BDA, denoted HIG+, was observed after the removal of PDF directions by *c.* 250°C, and was unblocked upon heating to 450–490°C. HIG+ directions have steep and positive inclinations in three samples (Fig. 3; Table 1), whereas these directions display much shallower inclinations in the remainder of samples, suggesting that they may not be adequately separated from PDF. The HIG+ component seen in site BDB (Fig. 3; Table 1) unblocked at temperature *c.* 500°C after the removal of a PDF component. The ChRM at site BDD is steeply inclined like HIG+, but is of opposite polarity and therefore denoted HIG− (Fig. 3; Table 1). Demagnetization of sites BDA, BDB, BDC and BDD above 530°C revealed no further consistent magnetic directions. The unblocking-temperatures range of HIG+ suggests that this component is carried by magnetite.

4.b. Bhima Group

During the AF pretreatment and thermal demagnetization up to 200°C, all samples from the Katamdevarahalli Limestone (site BA) and Harwal Shale (site BB) of the Bhima Group in the Bhima Basin revealed a PDF component (Figs 4, 5; Table 1). Between 200°C and 300°C, an intermediate unblocking component (labelled INT2), which was not observed at Kaladgi sites, was identified as well-grouped W-oriented directions with positive inclinations (Figs 4, 5; Table 1). The steep-downwards directed ChRM at site BA (i.e. HIG+ component) was present in all samples (Figs 4, 5) and unblocked in the temperature interval of 425–450°C or 490–500°C. Further demagnetization of BA samples revealed no consistent components. At site BB, samples revealed a component that is near antipodal to INT1+ between thermal steps of *c.* 250°C and *c.* 475°C, and therefore denoted INT1− (Figs 4, 5; Table 1). INT− represents the most stable component (ChRM) in six samples. In the remainder of samples the ChRM corresponds to HIG+, which is unblocked at temperature *c.* 500°C after the removal of INT− (Table 1). As in the Kaladgi Basin, the magnetic carrier of the HIG+ component here is interpreted to be magnetite.

5. Timing of magnetizations

5.a. INT1+/- and INT2 magnetizations

The INT2 magnetization (Figs 5, 6; Table 1) was isolated in the Bhima Group (sites BA and BB) as a low-coercivity component superimposed on the ChRM (i.e. the HIG+/- component). INT2 is reminiscent of an overprint (i.e. A magnetization) identified by De Kock *et al.* (2015) in Sequence III limestone of Pranhita–Godavari and Chattisgarh basins further NE of our study area. Similarly, the INT2 pole overlaps with the A pole of De Kock *et al.* 2015 (Fig. 7; Table 2). De Kock *et al.* (2015) interpreted their A magnetization to most likely represent a 1.0 Ga overprint.

The INT1+ magnetization was identified as the most stable component (ChRM) at site BDC, but was removed before HIG− at site BDD (Fig. 3; Table 1). INT1− was removed before HIG+ at site BB (Fig. 5; Table 1). Note that INT+ and INT− were never observed in the same sample. The INT1+/- pole is comparable to a widespread Ediacaran–Cambrian overprint (Fig. 7; Table 2) in India (e.g. Goutham *et al.* 2006; Pradhan *et al.* 2008; Belica *et al.* 2014; Pivarunas *et al.* 2019).

5.b. HIG+/- magnetization

The HIG+/- magnetization displays both positive (4 sites, 19 samples) and negative (1 site, 5 samples) inclinations (Fig. 6) on

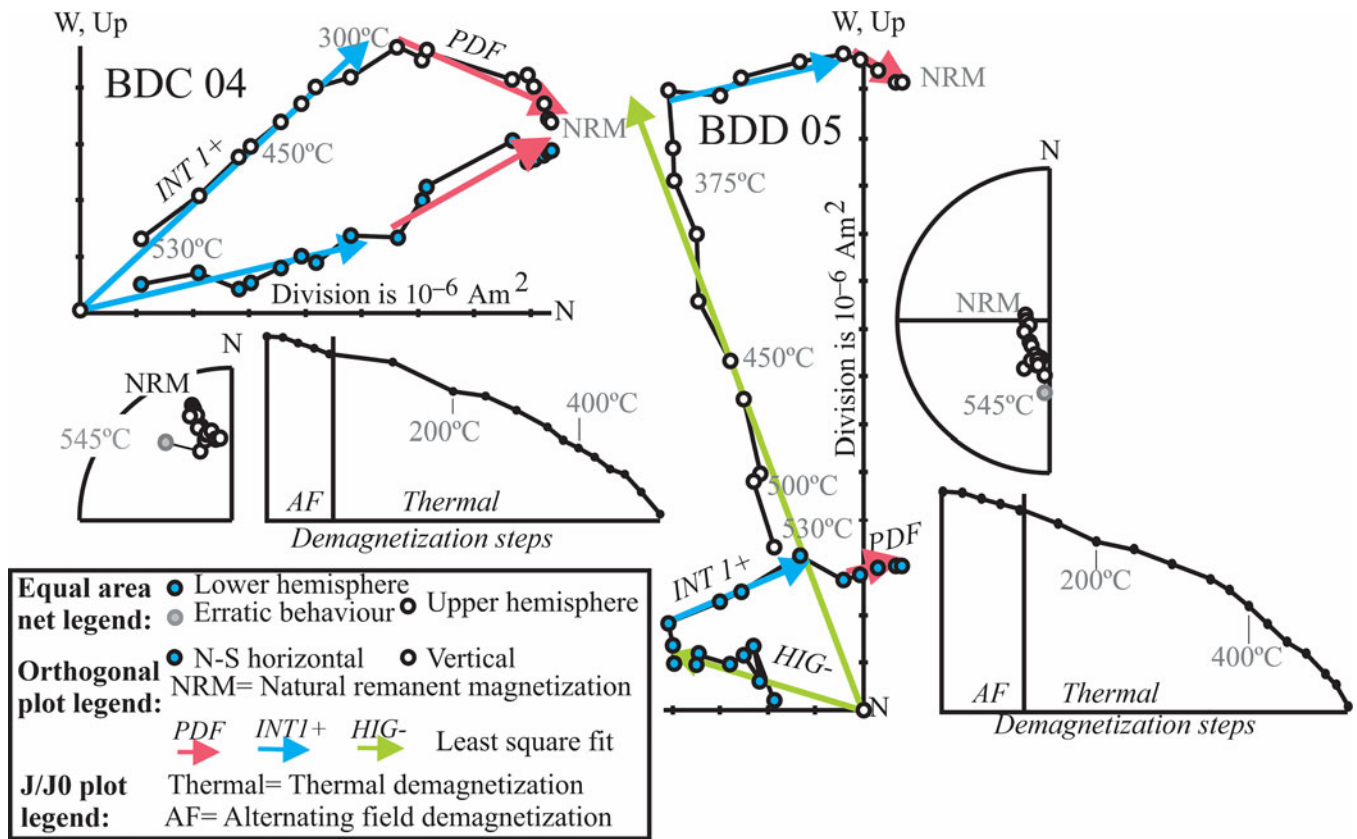


Fig. 2. Examples of demagnetization behaviour of Konkankoppa Limestone (BDC) and Halkurki Shale (BDD) of the Badami Group of the Kaladgi Basin represented as orthogonal projection onto the horizontal and E-W vertical planes, as well as on equal-area diagrams (both in geographic coordinates) obtained after demagnetization steps.

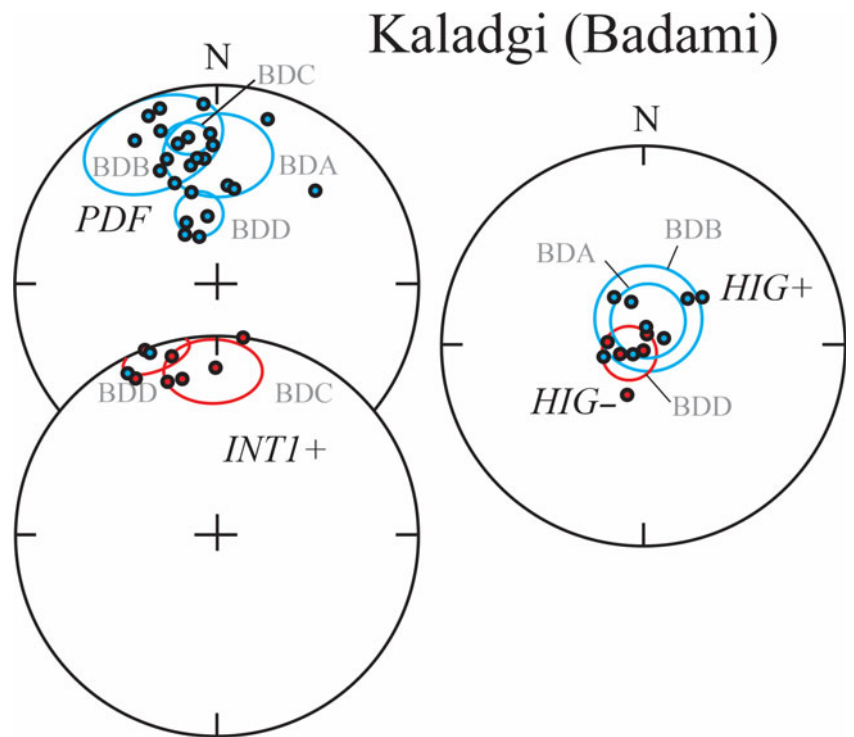


Fig. 3. Summary of various magnetic components from Konkankoppa Limestone (BDA and BDC) and Halkurki Shale (BDB and BDD) of the Badami Group of the Kaladgi Basin. The blue (red) circles are α_{95} confidence circles about the mean with positive (negative) inclination. Following the removal of the poorly resolved present-day field (PDF), INT1+ components were identified at 250–300°C at site BDD and at 475–530°C at site BDC. At higher temperature demagnetization steps (i.e. 450–490°C or 500–530°C), sites BDA, BDB and BDD revealed either steep downwards-directed (HIG+) or upwards-directed (HIG-) ChRMs.

Table 1. Summary of identified magnetic components.

Site	Latitude (°N)	Longitude (°E)	No. samples included in mean (<i>n</i>)/ No. samples drilled at site (<i>N</i>)	Declination (°)	Inclination (°)	Precision parameter, <i>k</i>	Cone of 95% confidence, α_{95}
Component PDF (unblocks at 200–250°C): identified in all Kaladgi and Bhima sites							
BDA	16.1	75.9	7/8	0.7	34.6	9.0	19.5
BDB	16.1	75.9	3/8	335.8	21.2	18.3	24
BDC	16.2	76.5	6/9	346.2	60.5	44.9	9.2
BDD	16.3	75.2	8/8	349.3	26.1	50.1	7.4
BA	16.7	76.3	7/7	4.6	27.8	25.2	11.3
BB	16.5	76.4	8/9	350.1	24.3	114.9	4.9
Component PDF mean (5 sites included; site BDB excluded)				354.8	34.7	25.1	15.5
Component INT1+/-: unblocks in Kaladgi sites at 250–300°C or 500–530°C and in one Bhima site (BB) at 425°C–475°C							
BDC	16.2	76.5	4/9	354.1	–14.7	18.9	16.9
BDD	16.3	75.2	5/8	343.6	–6.9	30.0	12.7
BB	16.5	76.4	6/9	165.5	–10	12.6	17.8
Component INT1+/- mean (3 sites included)				347.7	–3.9	34.7	21.2
Component INT2 (unblocks at c. 300°C): exclusively identified in Bhima sites							
BA	16.7	76.3	5/7	288.7	72.5	160.5	5.4
BB	16.5	76.4	6/9	284.1	67.4	405.5	3
Component INT2 mean (2 sites included)				286.1	70.0	461.5	11.6
Component HIG+/- (present in all sites BDC): unblocks at 450–500°C, with maximum unblocking temperature c. 530°C							
BDA	16.1	75.9	3/8	8.7	79.9	40.2	15.2
BDB	16.1	75.9	5/8	8.5	78.9	8.3	21.4
BDD	16.3	75.2	5/8	244	–83.2	18.3	11.1
BA	16.7	76.3	7/7	134.1	81.7	200.4	4.6
BB	16.5	76.4	4/9	218.6	84.6	14.6	21.4
Component HIG+/- mean (5 sites included)				40.5	86.3	87.0	8.2

PDF – present-day field.

which we were able to perform a reversal test. When the reversal test of McFadden & McElhinny (1990) is applied on site means, the result is positive class ‘B’ (observed angle, $\gamma_o = 4.67^\circ$ and critical angle, $\gamma_c = 6.96^\circ$). The reversal test is positive class ‘C’ at sample level ($\gamma_o = 5.39^\circ$ and $\gamma_c = 14.12^\circ$). A positive reversal test has been used in multiple studies (e.g. Bates & Jones, 1996; Bohnel, 1999; Goutham *et al.* 2006; Pradhan *et al.* 2008; Letts *et al.* 2010; Pisarevsky *et al.* 2013) to argue for the primary nature of magnetization in the absence of field tests, although remagnetization can also produce dual polarity results (e.g. Evans *et al.* 2002; De Kock *et al.* 2015; Humbert *et al.* 2017). In this study, the presence of distinctly different palaeomagnetic directions in sampling sites and the dissimilarity of HIG+/- to younger magnetizations in India could argue against a pervasive remagnetization of the sampling area. It is therefore most likely that the HIG+/- remanence was recorded during or just after the deposition of the studied carbonates.

A HIG+/- mean was calculated after all data were inverted to single polarity (i.e. positive inclination). Keeping in mind that the limited number of samples of the study (of the total of 49 samples, 24 had HIG+/- magnetization) detracted from the general cluster of directional groupings, the following conditions were considered for mean calculation: (1) the site mean is based on three or more

samples; (2) Fisher’s (1953) precision parameter *k* for the site mean is > 8 ; and (3) the radius of the cone of 95% confidence about the mean, $\alpha_{95} < 21.5^\circ$.

The HIG+/- mean (declination, $D = 40.49^\circ$; inclination, $I = 86.32^\circ$; $\alpha_{95} = 8.24^\circ$) was used to calculate a palaeopole at latitude $\lambda = 21.67^\circ$ N and longitude $\phi = 81.06^\circ$ E with an A_{95} of 15.9° . This pole fulfils four of the seven quality criteria ($Q = 4$) for palaeomagnetic poles (Van der Voo, 1990). Quality criteria not satisfied are (1) criterion 1, because there is uncertainty about the age of the studied carbonates; (2) criterion 2, because our pole is based on 24 samples and therefore falls short of the required > 24 samples; and (3) criterion 4, because the HIG+/- pole is not constrained by palaeomagnetic field tests.

6. Discussion

In order to investigate the possible timing of deposition of Sequence III carbonate successions in the Badami and Bhima groups, our HIG+/- palaeopole is plotted along with selected existing Meso- to Neoproterozoic palaeopoles from the southern Indian Shield (Fig. 7; Table 2). Such a comparison reveals that our pole is different from the pole for the c. 1.4 Ga Lakna dyke

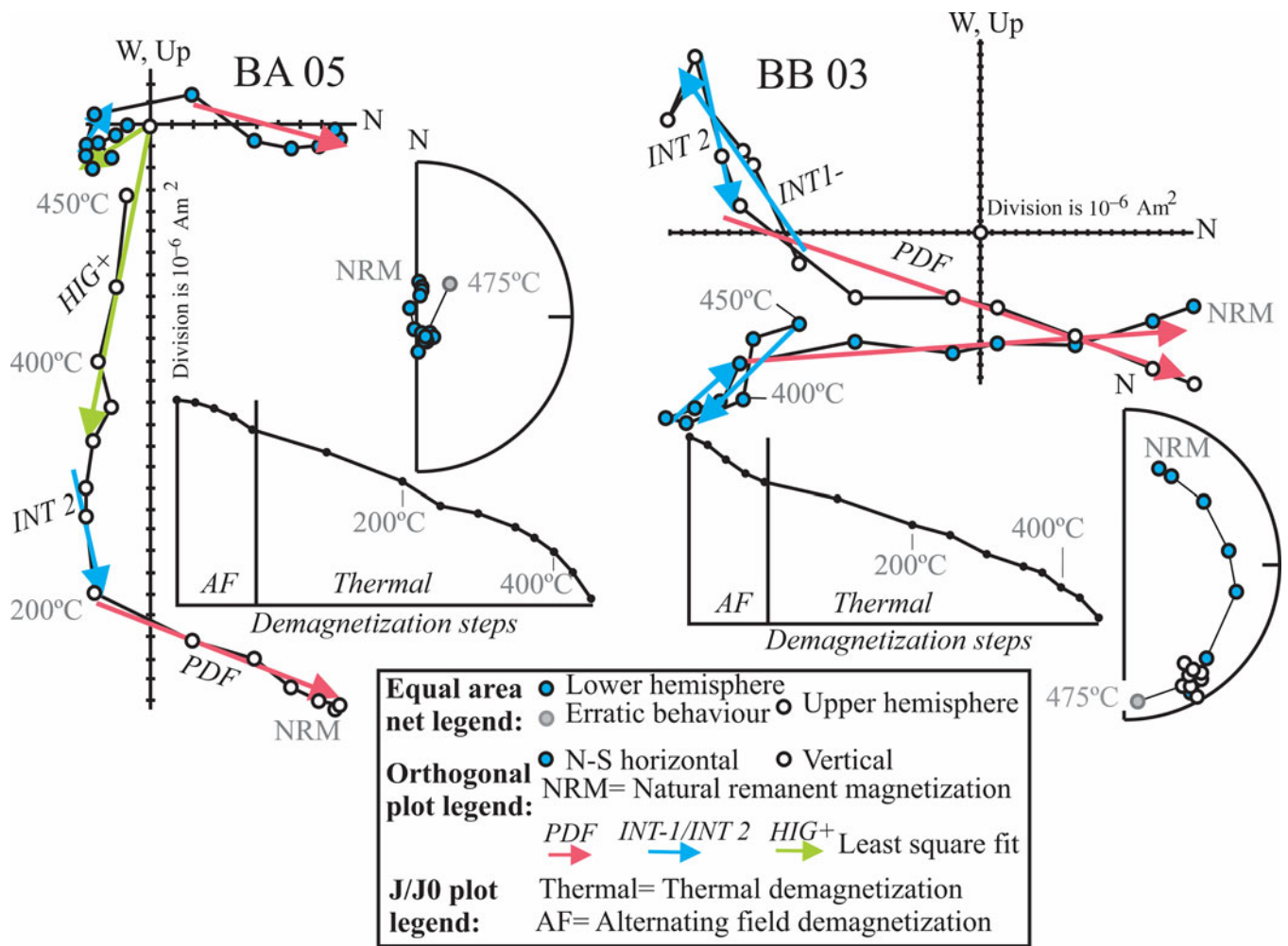


Fig. 4. Examples of demagnetization behaviour of samples from the Katamdevarahalli Limestone (BA) and Harwal Shale (BB) of the Bhima Group, represented as orthogonal projection onto the horizontal and E-W vertical planes as well as on equal-area diagrams (both in geographic coordinates) obtained after demagnetization steps.

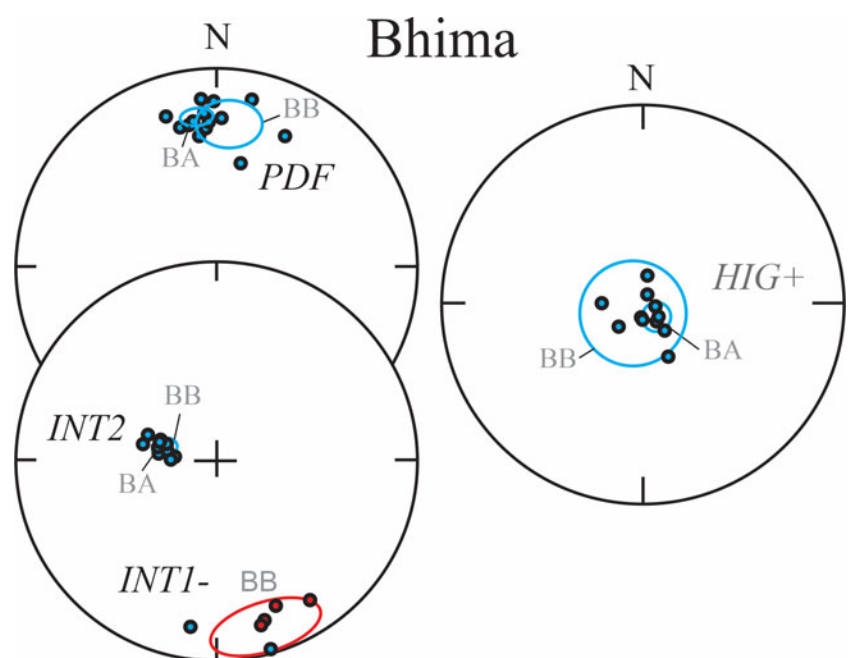


Fig. 5. Summary of various magnetic components of the Katamdevarahalli Limestone (BA) and Harwal Shale (BB) in the Bhima Group. The blue (red) circles are α_{95} confidence circles about the mean with positive (negative) inclination. Following the removal of the present-day field (PDF), INT2 directions were revealed at 200–300°C. During demagnetization steps up to 425–450°C, an HIG+ component was identified at site BA. At this temperature range, site BB revealed an INT1- component that is apparently antipodal to INT+ of Kaladgi samples. Subsequent demagnetization of some BB samples up to steps 500–505°C revealed a HIG+ component.

Kaladgi (Badami) and Bhima

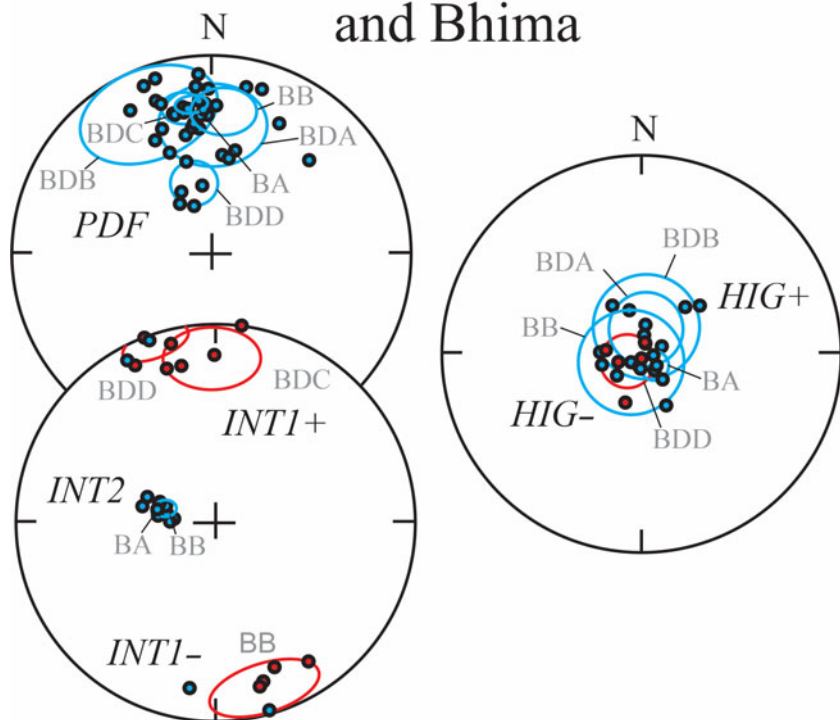


Fig. 6. Summary of various magnetic components obtained from the Sequence III carbonates in the Kaladgi (Badami Group) and Bhima (Bhima Group) basins. The blue (red) circles are α_{95} confidence circles about the mean with positive (negative) inclination.

swarm (Pisarevsky *et al.* 2013) and the *c.* 1.1 Ga and younger Indian poles (e.g. Gregory *et al.* 2006; Malone *et al.* 2008; Pradhan *et al.* 2012). However, it largely overlaps with the HAR pole of the Harahalli alkaline dyke swarm (Radhakrishna & Mathew 1996; Pradhan *et al.* 2008). This is a very interesting observation because the HAR pole, previously considered to be of age *c.* 823 Ma (e.g. Li *et al.* 2004; Maloof *et al.* 2006) based on the 800–850 Ma Rb–Sr and K–Ar ages obtained by Ikramuddin & Stueber (1976) and Kumar *et al.* (1989) from individual Harahalli dykes, has more recently been suggested to be older by *c.* 400 Ma (Pradhan *et al.* 2008). This age revision was based on a U–Pb 1192 ± 10 Ma estimate obtained from laser ablation multicollector inductively coupled plasma mass spectrometry (LA-MC-ICP-MS) dating of zircon crystals extracted from one of the Harahalli dykes. If this new age for the Harahalli dyke swarm is accepted, it may well imply that the Badami and Bhima groups are Mesoproterozoic in age, as indicated by stratigraphic correlation of unconformity-bound sequences (Fig. 1b), rather than Neoproterozoic in age, as suggested by radiometric age data (e.g. Joy *et al.* 2018; Patil Pillai *et al.* 2018).

At this stage, it is perhaps worth noting that our HIG+/- pole for Sequence III carbonates in the Badami and Bhima groups is close to the C+/- pole that De Kock *et al.* (2015) delineated from Sequence III carbonates in the Pranhita–Godavari (Penganga Group) and Chattisgarh (Raipur Group) basins to the east (Figs 1b, 7). The C+/- pole is very robust in that it is based on > 24 samples, is of dual polarity, and is supported by a positive intra-formational conglomerate test and a regional fold test. The close proximity of our HIG+/- pole to the C+/- pole (Fig. 7) most likely indicates a minimal apparent polar wander during the acquisition of the concerned magnetizations.

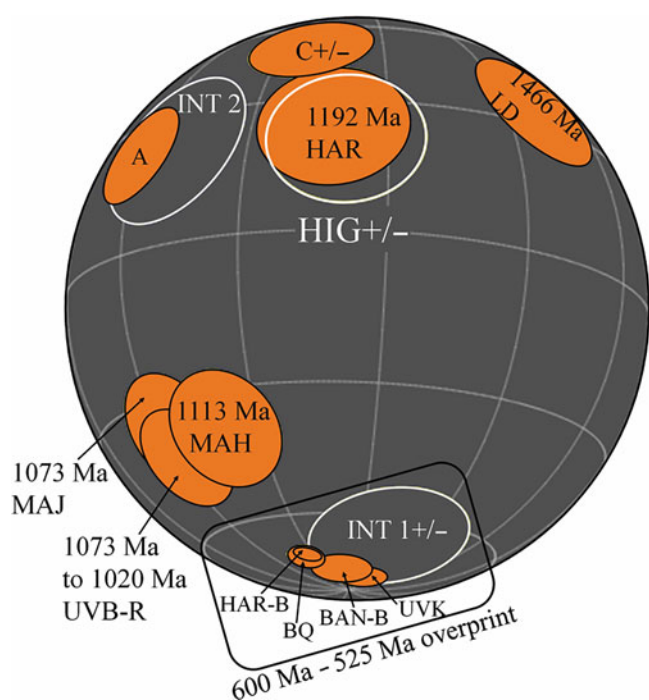
Although by far not definitive, the above indications that the Bhima and Badami successions are late Mesoproterozoic in age

certainly validate a critical evaluation of the data that led to assignment of a Neoproterozoic age for these successions. The later age assignment is based on essentially three assumptions, namely (1) that the Rb–Sr ages of 798–813 Ma (Joy *et al.* 2018) obtained from glauconite-bearing sandstone of the Bhima Group represent a depositional age; (2) that a dyke dated to give an $^{40}\text{Ar}/^{39}\text{Ar}$ age of *c.* 1154 ± 4 Ma is older than the Badami Group of the Kaladgi Basin (Patil Pillai *et al.* 2018); and (3) that detrital diamonds present in conglomerates along the basal erosional unconformity of Sequence III were derived from the diamondiferous Raichur and Wajrakarur Kimberlites fields of age *c.* 1100 Ma (Chalapathi Rao *et al.* 2010) further to the south (e.g. Collins *et al.* 2015).

Firstly, the suggestion that the *c.* 800 Ma Rb–Sr glauconites are of primary depositional origin (Joy *et al.* 2018) appear to be rather dubious. The main reason for this is that it is not clear how these ages are brought in line or explained by the U–Pb age of *c.* 0.96 Ga and the Th–Pb age of 0.91 ± 0.13 Ga obtained by the same authors on limestone beds in the succession. A more logical interpretation may be that this discrepancy indicates that the glauconite ages were reset *c.* 800 Ma after deposition of the limestones. Also, the detrital zircon age populations obtained from the basal quartzites of the successions are difficult to place in the context of a Neoproterozoic age. The youngest near-concordant zircons have ages of 2.2–2.3 Ga with no indication of any zircons having been derived from very late Mesoproterozoic or early Neoproterozoic provenance. This is despite the fact that (1) one of the main periods of orogenesis along the Central Indian Tectonic Zone, which resulted in the amalgamation of the northern and southern cratonic blocks of India situated to the north of the Purana basins, was at 0.975 ± 0.067 Ga (Chatterjee & Ghose, 2001); and (2) palaeocurrents measured by Joy *et al.* (2018) in the basal quartzite of the Badami Group have a major mode indicating transport from the NE. The U–Pb systems from which the 0.96 Ga ages were obtained on carbonates of the Bhima and Badami groups

Table 2. Selected Indian palaeopoles and palaeopoles from this study

Approximate pole age (Ma)	Rock unit	Pole name	Latitude (° N)	Longitude (° E)	Oval of 95% confidence (dp, dm) or A_{95}	Reference
525–600	Harrohali I5150 overprint B	HAR-B	–72.2	56.1	(1.9, 3.8)	Pradhan <i>et al.</i> (2008)
525–600	Bangalore dyke overprint B	BAN-B	–78.8	77.3	6	Halls <i>et al.</i> (2007)
525–600	Banganapalli Quartzite	BQ	–73.4	53.7	(2.6, 5.2)	Goutham <i>et al.</i> (2006)
525–600	Kaladgi and Bhima basins (INT1+/- component)	INT1+/-	–68.0	110.6	12.7	This study
1020–1073	Bhandar and Rewa groups	UVB-R	–43	32.5	11	Malone <i>et al.</i> (2008)
1073 ± 13.7	Majhgawan Kimberlite	MAJ	–36.8	32.5	(9, 16.6)	Gregory <i>et al.</i> (2006)
1113 ± 7	NW–SE Mahoba dykes	MAH	–38.7	49.5	(9.5, 16.3)	Pradhan <i>et al.</i> (2012)
1100–1200	P-G and Chattisgarh basins (A component)	A	22.8	28.1	10.8	De Kock <i>et al.</i> (2015)
1100–1200	Bhima basin (INT2 component)	INT2	22.8	38.6	17.3	This study
1100–1200	P-G and Chattisgarh basins (C+/- component)	C+/-	50.1	67.4	12.4	De Kock <i>et al.</i> (2015)
1100–1200	Kaladgi and Bhima basins (HIG+/- component)	HIG +/-	21.7	81.1	15.9	This study
1192 ± 10	Harrohali alkaline dykes	HAR	24.9	78	15	Pradhan <i>et al.</i> (2008)
1466.4 ± 2.6	Lakhna dykes	LD	36.6	132.8	(12.4, 15.9)	Pisarevsky <i>et al.</i> (2013)

**Fig. 7.** Palaeopoles obtained from this study (white) compared with existing palaeopoles in India (orange). See Table 2 for pole details.

also appeared rather disturbed, so much so that Joy *et al.* (2018) considered them as derived from isotopic exchange between different fluids. Although not considered as an option by Joy *et al.* (2018), it may well be that this exchange took place during the *c.* 0.975 Ga orogenesis in the Central Indian Tectonic Zone.

Secondly, the suggestion by Patil Pillai *et al.* (2018) that the Badami Group is younger than the *c.* 1154 Ma mafic dyke that they described is also problematic. The only known outcrops of that dyke are from a small synclinal structure comprising upper strata of the Kaladgi Basin. However, the topmost beds of the Group have been removed by recent erosion in the syncline, so there is no direct geological evidence available that the dyke is actually cut by the unconformity at base of the Badami Group. It is therefore quite possible that this dyke could also have transected the strata of the Badami Group that have since been eroded. Even if follow-up mapping would indicate that the dyke of Patil Pillai *et al.* (2018) may actually be disconformably overlain by the Badami Group somewhere along its extension, then their $^{40}\text{Ar}/^{39}\text{Ar}$ age of *c.* 1154 Ma should also be considered with care. It is important to realize that this age was obtained using the whole-rock method. According to previous studies (e.g. Bernard-Griffiths, 1989), the geochemical and geological conditions for a whole-rock sample to represent a primary age is rarely fulfilled by older mafic dykes. Patil Pillai *et al.* (2018) noted that the dyke was affected by weathering as well as metamorphism. Among the secondary mineral phases that formed from primary minerals, these authors reported the presence of secondary hornblende and actinolite that replace the magmatic pyroxene. The whole-rock $^{40}\text{Ar}/^{39}\text{Ar}$ dating therefore involved mixed primary and second generations of K-minerals. Perhaps a more cautious approach should be taken and the *c.* 1154 Ma result regarded as the minimum age and not the crystallization age of the dyke.

Thirdly, there is also no geological evidence that the detrital diamonds present in the basal conglomerates of Sequence III were actually sourced from the diamondiferous kimberlite fields of age *c.* 1.1 Ga further to the south. These kimberlites intrude basement granitoids of the Dharwar craton (e.g. Crawford & Compton, 1973), and again there are no known localities where proper

contact relationships with strata of either the Badami–Bhima successions or the upper units of the Cuddapah Basin are exposed. In this regard, it is also interesting to note that Dongre *et al.* (2008) described xenoliths of limestone in the kimberlite of the Siddanpalle cluster of the Raipur kimberlite field. These xenoliths are similar in appearance to the carbonates of the Badami and Bhima groups. Dongre *et al.* (2008) therefore suggested that these successions could well be older than 1.1 Ga, the age of the kimberlites.

7. Summary and conclusion

New palaeomagnetic results are reported from the carbonate units of the Badami and Bhima groups, tentatively correlated on stratigraphic grounds with unconformity-bound Sequence III in the upper parts of the Purana successions across the southern Indian Shield. A new pole position is obtained from these carbonates (HIG+/- magnetization) at latitude 21.7° N, longitude 81.1° E, with an A_{95} of 15.9°. The HIG+/- magnetization is considered primary based on (1) its dissimilarity to known younger magnetizations in India; (2) the presence of distinctly different palaeomagnetic components at various sites; and (3) a positive reversal test. Our pole differs from the *c.* 1.4 Ga pole and various *c.* 1.1 Ga and younger Indian poles, but overlaps with the pole of the Harohalli alkaline dykes. The age of the Harohalli dyke pole was recently revised to *c.* 1.2 Ga (based on a U–Pb age of $c.$ 1192 ± 10 Ma from one of the Harahalli dykes using LA-MS-ICP-MS on zircon), and not to 800–850 Ma as initially suggested from Rb–Sr and K–Ar whole-rock datings. On this basis, a Mesoproterozoic age can be interpreted for the studied carbonates, contrary to the generally interpreted Neoproterozoic age. Critical evaluation of the parameters from which the earlier Neoproterozoic age was established indicates that some were based on assumptions for which there is no direct stratigraphic field evidence, and that the available Rb–Sr and U–Pb ages on glauconites and limestone in the Badami and Bhima groups could be related to later alteration events rather than representing depositional ages. It may therefore be possible that the studied carbonates correlate laterally both in time and space with unconformity-bound Sequence III of the Purana successions. It implies that this virtually undeformed succession was deposited as a sheet of deep-water, including pelagic, carbonates over much of the southern Indian Shield area during late Mesoproterozoic times. However, our results are not fully definitive and further studies are required to refine them. Such studies should include sampling of more sites for palaeomagnetic research in the Bhima and Badami groups, as well as in other basins such as the Cuddapah Basin, combined as far as possible with radiometric age studies.

Conflict of interest. None

Acknowledgements. This research project, initiated by Professors NJ Beukes and VS Hegde, benefited from a Raman Fellowship scheme. The support of the DSI-NRF Centre of Excellence for Integrated Mineral and Energy Resource Analysis (DSI-NRF CIMERA) is also acknowledged. Opinions expressed and conclusions arrived at are those of the author(s), and are not necessarily to be attributed to the Centre of Excellence. HW also acknowledges financial contributions from the Paleoproterozoic Mineralization Research Group at the University of Johannesburg in South Africa. Professor J Mukhopadhyay is thanked for fruitful discussions about the geology of the Proterozoic Purana basins. We thank Professor S Patranabis-Deb for inviting us to contribute to this thematic issue of the *Geological Magazine*, and for handling the review process.

Professor J Meert and two anonymous referees are thanked for their constructive criticisms and suggestions, which greatly improved the manuscript.

References

- Bates PM and Jones DL (1996) A palaeomagnetic investigation of the Mashonaland dolerites, north-east Zimbabwe. *Geophysical Journal International* **126**, 513–24.
- Belica ME, Piispa EJ, Meert JG, Pesonen L, Plado J, Manoj J, Pandit K, Kamenov GD and Celestino M (2014) Paleoproterozoic mafic dyke swarms from the Dharwar craton; paleomagnetic poles for India from 2.37 to 1.88 Ga and rethinking the Columbia supercontinent. *Precambrian Research* **244**, 100–22.
- Bernard-Griffiths JB (1989) The rubidium-strontium method. In *Nuclear 327 Methods of Dating* (eds E Roth and B Poty), pp. 73–94. New York: Kluwer Academic Publishers.
- Bickford ME, Basu A, Patranabis-Deb S, Dhang PC and Schieber J (2011) Depositional history of the Chattisgarh Basin, Central India: constraints from new SHRIMP zircon ages. *The Journal of Geology* **119**, 33–50.
- Bohnel H (1999) Paleomagnetic study of Jurassic and Cretaceous rocks from the Mixteca terrane (Mexico). *Journal of South American Earth Sciences* **12**, 545–56.
- Chakraborty PP, Dey S and Mohanty SP (2010) Proterozoic platform sequences of Peninsular India: implications towards basin evolution and supercontinent assembly. *Journal of Asian Earth Sciences* **39**, 589–607.
- Chalapathi Rao NV, Anand M, Dongre A and Osborne I (2010) Carbonate xenoliths hosted by the Mesoproterozoic Siddanpalli Kimberlite Cluster (Eastern Dharwar craton): implications for the geodynamic evolution of southern India and its diamond and uranium metallogenesis. *International Journal of Earth Sciences* **99**, 1791–804.
- Chatterjee N and Ghose NC (2001) Extensive early Neoproterozoic high-grade metamorphism in North Chotanagpur Gneissic Complex of the Central Indian Tectonic Zone. *Gondwana Research* **20**, 362–79.
- Chaudhuri AK, Mukhopadhyay J, Patranabis-Deb S and Chanda SK (1999) The Neoproterozoic successions of peninsular India. *Gondwana Research* **2**, 213–25.
- Chaudhuri AK, Saha D, Deb GK, Patranabis-Deb S, Mukherjee MK and Gosh G (2002) The Purana basins of southern cratonic province of India: a case for Mesoproterozoic fossil rifts. *Gondwana Research* **5**, 23–33.
- Collins AS, Patranabis-Deb S, Alexander E, Bertram CN, Falster GM, Gore RJ, Mackintosh J, Dhang PC, Saha D, Payne JL, Jourdan F, Backé G, Halverson GP and Wade BP (2015) Detrital mineral age, radiogenic isotopic stratigraphy and tectonic significance of the Cuddapah Basin, India. *Gondwana Research* **28**, 1294–309.
- Conrad JE, Hein JR, Chaudhuri AK, Patranabis-Deb S, Mukhopadhyay J, Deb GK and Beukes NJ (2011) Constraints on the development of central India Proterozoic basins from $^{40}\text{Ar}/^{39}\text{Ar}$ analysis of authigenic glauconitic minerals. *GSA Bulletin* **123**, 158–67.
- Crawford AR and Compston W (1973) The age of the Cuddapah and Kurnool systems, southern India. *Journal of the Geological Society of Australia* **19**, 453–64.
- De Kock MO, Beukes NJ and Mukhopadhyay J (2015) Palaeomagnetism of Mesoproterozoic limestone and shale successions of some Purana basins in southern India. *Geological Magazine* **152**, 728–50.
- Dey S (2015) Geological history of the Kaladgi–Badami and Bhima basins, south India: Sedimentation in a Proterozoic intracratonic setup. In *Precambrian Basins of India: Stratigraphic and Tectonic Context* (eds R Mazumder and PG Eriksson), pp. 283–96. Geological Society of London, Memoir no. 43.
- Dongre A, Chalapathi Rao NV and Kamde G (2008) Limestone xenolith in Siddanpalli Kimberlite, Gadwal granite-greenstone terrain, eastern Dharwar craton, Southern India: remnant of Proterozoic platformal cover sequence of Bhima/Kurnool Age? *Journal of Geology* **116**, 184–91.
- Evans DAD, Beukes NJ and Kirschvink JL (2002) Paleomagnetism of a lateritic paleoweathering horizon and overlying Paleoproterozoic red beds from South Africa: Implications for the Kaapvaal apparent polar wander path and

- a confirmation of atmospheric oxygen enrichment. *Journal of Geophysical Research* **107**, 2326–33.
- Fisher RA** (1953) Dispersion on a sphere. *Proceedings of the Royal Society of London. Series A* **217**, 295–305.
- Goutham MR, Raghobabu K, Prasad CVRK, Subba Rao KV and Damodara Reddy V** (2006) A Neoproterozoic geomagnetic field reversal from the Kurnool Group, India: implications for stratigraphic correlation and formation of Gondwanaland. *Journal Geological Society of India* **67**, 221–33.
- Gregory LC, Meert JG, Pradhan V, Pandit MK, Tamrat E and Malone SJ** (2006) A paleomagnetic and geochronologic study of the Majhgawan kimberlite, India: implications for the age of the Upper Vindhyan Supergroup. *Precambrian Research* **149**, 65–75.
- Halls HC, Kumar A, Srinivasan R and Hamilton MA** (2007) Paleomagnetism and U-Pb geochronology of easterly trending dykes in the Dharwar craton, India: feldspar clouding, radiating dyke swarms and the position of India at 2.37 Ga. *Precambrian Research* **155**, 47–68.
- Humbert F, Sonnette L, De Kock MO, Robion P, Horng CS, Cousture A and Wabo H** (2017) Palaeomagnetism of the early Palaeoproterozoic, volcanic Hekpoort Formation (Transvaal Supergroup) of the Kaapvaal craton, South Africa. *Geophysical Journal International* **209**, 842–65.
- Ikramuddin M and Stueber AM** (1976) Rb-Sr ages of Precambrian dolerite and alkaline dykes, south-east Mysore State, India. *Lithos* **9**, 235–241.
- Jones CH** (2002) User-driven integrated software lives: “Paleomag” paleomagnetic analysis on the Macintosh™. *Computers and Geosciences* **28**, 1145–51.
- Joy S, Patranabis-Deb S, Saha D, Jelsma H, Maas R, Söderlund U, Tappe S, Gert Van Der Linde G, Banerjee A and Krishnan U** (2018) Depositional history and provenance of cratonic “Purana” basins in southern India: a multipronged geochronology approach to the Proterozoic Kaladgi and Bhima basins. *Geological Journal* **54**, 2957–79, doi: [10.1002/gj.3415](https://doi.org/10.1002/gj.3415).
- Kale VS and Phansalkar VG** (1991) Purana basins of peninsular India: a review. *Basin Research* **3**, 1–36.
- Kirschvink JL** (1980) The least-squares line and plane and the analysis of palaeomagnetic data. *Geophysical Journal of the Royal Astronomical Society* **62**, 699–718.
- Kirschvink JL, Kopp RE, Raub TD, Baumgartner CT and Holt JW** (2008) Rapid, precise, and high-sensitivity acquisition of paleomagnetic and rock-magnetic data: development of a low-noise automatic sample changing system for superconducting rock magnetometers. *Geochemistry, Geophysics and Geosystems* **9**, Q05Y01, doi: [10.1029/2007GC001856](https://doi.org/10.1029/2007GC001856).
- Kumar A, Sivaraman TV, Bhaskararao YJ and Gopalan K** (1989) Rb-Sr ages of two dyke swarms from the Dharwar craton, Karnataka (abstract). In *Nuclear Methods of Dating* (eds E Roth and B Poty), pp. 73–104. Netherlands: CEA.
- Letts S, Torsvik TH, Webb SJ and Ashwal LD** (eds) (2010) New Palaeoproterozoic palaeomagnetic data from the Kaapvaal Craton. In *The Formation and Evolution of Africa: A Synopsis of 3.8 Ga of Earth History* (eds DJJ van Hinsbergen, SJH Buitert, TH Torsvik, C Gaina and SJ Webb), pp. 9–26. Geological Society of London, Special Publication no. 357.
- Li Z, Evans D and Zhang S** (2004) A 90° spin on Rodinia: Possible causal links between the Neoproterozoic supercontinent, superplume, true polar wander and low-latitude glaciation. *Earth and Planetary Science Letters* **220**, 409–21.
- Malone SJ, Meert JG, Banerjee S, Pandit MK, Tamrat E, Kamenov GD, Pradhan VR and Sohl LE** (2008) Paleomagnetism and detrital zircon geochronology of the Upper Vindhyan sequence, Son Valley and Rajasthan, India: A ca. 1000 Ma closure age for the Purana basins? *Precambrian Research* **164**, 137–59.
- Maloof AC, Havlorsen GP, Kirschvink JL, Schrag DP, Weiss BP and Hoffman PF** (2006) Combined paleomagnetic, isotopic, and stratigraphic evidence for true polar wander from the Neoproterozoic Akademikerbreen Group, Svalbard, Norway. *Geological Society of America Bulletin* **118**, 1099–124.
- McFadden PL and McElhinny MW** (1990) Classification of the reversal test in palaeomagnetism. *Geophysical Journal International* **103**, 725–29.
- Meert JG and Pandit MK** (2015) The Archaean and Proterozoic history of Peninsular India: tectonic framework for Precambrian sedimentary basins in India. In *Precambrian Basins of India: Stratigraphic and Tectonic Context* (eds R Mazumder and PG Eriksson), pp. 29–54. Geological Society of London, Memoir no. 43.
- Mukhopadhyay J and Chaudhuri AK** (2003) Stratigraphy of the Chanda Limestone from the Proterozoic Penganga Group, Adilabad, Andhra Pradesh, India: Implications for understanding depositional setting and palaeogeography. *Journal of the Geological Society of India* **62**, 356–68.
- Patil Pillai S, Pande K and Kale VS** (2018) Implications of new ⁴⁰Ar/³⁹Ar age of Mallapur Intrusives on the chronology and evolution of the Kaladgi Basin, Dharwar Craton. *Journal of Earth System Science* **127**, 32, doi: [10.1007/s12040-018-0940-5](https://doi.org/10.1007/s12040-018-0940-5).
- Patranabis-Deb S, Bickford ME, Hill B, Chaudhuri AK and Basu A** (2007) SHRIMP ages of zircon in the uppermost tuff in Chattisgarh Basin in Central India require 500 Ma adjustment in Indian Proterozoic Stratigraphy. *The Journal of Geology* **115**, 407–15.
- Patranabis-Deb S, Saha D and Tripathy V** (2012) Basin stratigraphy, sea-level fluctuations and their global tectonic connections: evidence from the Proterozoic Cuddapah Basin. *Geological Journal* **47**, 263–83.
- Pisarevsky SA, Biswal TK, Wang XC, Dewaele B, Ernst RE, Söderlund U, Tait JA, Ratte K, Singh YK and Cleve M** (2013) Palaeomagnetic, geochronological and geochemical study of Mesoproterozoic Lakhna Dykes in the Bastar Craton, India: implications for the Mesoproterozoic supercontinent. *Lithos* **174**, 125–43.
- Pivarunas AF, Meert JG, Pandit MK and Sinha A** (2019) Paleomagnetism and geochronology of mafic dykes from the Southern Granulite Terrane, India: Expanding the Dharwar craton southward. *Tectonophysics* **760**, 4–22.
- Pradhan VR, Meert JG, Pandit MK, Kamenov G and Mondal MEA** (2012) Paleomagnetic and geochronological studies of the mafic dyke swarms of Bundelkhand craton, central India: Implications for the tectonic evolution and paleogeographic reconstructions. *Precambrian Research* **198–199**, 51–76.
- Pradhan VR, Pandit MK and Meert JG** (2008) A cautionary note on the age of the paleomagnetic pole obtained from the Harohalli dyke swarms, Dharwar craton, southern India. In *Indian Dykes* (eds RK Srivastava, C Sivaji and NVC Rao), pp. 339–52. New Delhi, India: Narosa Publishing House.
- Radhakrishna T and Joseph M** (1996) Late Precambrian (850–800 Ma) paleomagnetic pole for the south Indian shield from the Harohalli alkaline dykes: geotectonic implications for Gondwana reconstructions. *Precambrian Research* **80**, 77–87.
- Saha D, Patranabis-Deb S and Collins AS** (2016) Proterozoic stratigraphic of Southern India cratons and global context. In *Stratigraphy and Timescales* (ed. M Montanari), Volume **1**, pp. 1–59. Amsterdam: Elsevier.
- Van Der Voo R** (1990) The reliability of paleomagnetic data. *Tectonophysics* **184**, 1–9.
- Williams S, Müller RD, Landgrebe TCW and Whittaker JM** (2012) An open-source software environment for visualizing and refining plate tectonic reconstructions using high resolution geological and geophysical data sets. *GSA Today* **22**(4–5), doi: [10.1130/GSATG139A](https://doi.org/10.1130/GSATG139A).